Computational and Theoretical Chemistry 983 (2012) 95–100

Contents lists available at SciVerse ScienceDirect

Computational and Theoretical Chemistry

journal homepage: www.elsevier.com/locate/comptc

The degree of proton transfer for $XH\cdots NH_3$ (X = F, Br, HS, and HCOO) heterodimers upon attachment of an excess electron

Lihua Dong [a,b,*], Jinhu Wang [c]

[a] School of Chemical Engineering, Taishan Medical University, Taian, Shandong 271000, China
[b] Key Laboratory of Adaptation and Evolution of Plateau Biota, Northwest Institute of Plateau Biology, Chinese Academy of Sciences, Xining, Qinghai 810001, China
[c] School of Chemistry and Chemical Engineering, Shandong University, Jinan, Shandong 250100, China

ARTICLE INFO

Article history:
Received 14 September 2011
Received in revised form 14 December 2011
Accepted 9 January 2012
Available online 18 January 2012

Keywords:
Excess electron
Barrier-free proton transfer (BFPT)
Vertical detachment energy (VDE)
Potential energy surfaces (PESs)

ABSTRACT

A DFT method is employed to elucidate the degree of proton transfer (PT) for $XH\cdots NH_3$ (X = F, Br, HS, and HCOO) heterodimers upon an excess electron attachment. Only the anionic complex of $(BrH\cdots NH_3)^-$ has an intermolecular barrier-free proton transfer (BFPT) with a larger vertical detachment energy (VDE) of 16.60 kcal/mol. The anionic complexes without BFPT have only one ($F{-}H\cdots NH_3^-$ and $HCOO{-}H\cdots NH_3^-$) or two minima ($HS{-}H\cdots NH_3^-$ and $HS{-}NH_4^+$) in the potential energy surfaces (PESs). In the latter case, there is a transition state with an energy barrier of 1.76 kcal/mol. When solvent is considered as the environmental conditions, intermolecular PT occurs for anionic complexes of $(H_2O)_n(FH\cdots NH_3)^-$ and $(H_2O)_n(HCOOH\cdots NH_3)^-$. The minimum number of water molecules is three for the former and two for the latter respectively.

1. Introduction

The influence of an excess electron attachment has been an important issue in chemistry and biology for several decades [1–7]. In biology, attachment of an excess electron to DNA or RNA would result in mutagens [1]. In chemistry, the suspended excess electron could affect the intramolecular or intermolecular structural parameters [2], or provide extra stability for neutral complexes [3]. In the past years, people found that the excess electron could act as a driving force to induce barrier-free proton transfer (BFPT) in many reactions [7–12]. Moreover, intermolecular PT has been involved in the reactions of acids and bases, which, according to the Lowry–Brønsted theory, are the proton donors and proton acceptors, respectively [13].

As an excellent work described by Gutowski et al., electron-driven acid–base chemistry in $ClH\cdots NH_3$ complex had been investigated in details [14]. It was known that no appreciable PT occurred for the neutral ($ClH\cdots NH_3$) dimer [15]. In other words, ammonia (NH_3) and hydrogen chloride (HCl) cannot react under isolated condition [16]. In addition, the ability of excess electron attachment for PT is determined by the electrostatic dipole potential of the neutral cluster [17]. In fact, due to the excess electron in ($ClH\cdots NH_3$) system, PT occurs from molecule HCl to NH_3, where the excess electron is localized [14]. The computational dipole moment for ($ClH\cdots NH_3$) systems varies from 4.15 to 9.82 D upon the intermolecular PT, indicating the formation of $Cl^-NH_4^+$. The driving force for PT is employed to stabilize the excess negative charge on Rydberg orbitals of NH_3. The final structure could be described as $(Cl^-NH_4^+)^-$, which is characterized as the value of vertical detachment energy (VDE) (0.51 ev) upon intermolecular PT at CCSD(T) level. A significant value of VDE is a consequence of intermolecular PT to the group where unpaired electron is localized [6,10], and smaller values of VDE correspond to chemically untransformed structures, in which no PT occurs [18]. So, the VDE value can be used to assess the ability of the anion with respect to the neutral structure [10,12].

In the work done by Gutowski et al., only HCl was considered. For other acids (HX), such as hydrogen fluorine (HF), hydrogen bromine (HBr), sulfureted hydrogen (H_2S), and formic acid (HCOOH), no calculations were carried out systematically. In this work, calculations were performed in order to investigate the interaction of HX with NH_3 upon attachment of an excess electron. The degree of PT in $XH\cdots NH_3$ (X = F, Br, HS, and HCOO) heterodimers upon an electron attachment was studied. For the same purpose, water, as an environmental factor, was also considered in systems $XH\cdots NH_3$ (X = F, HCOO).

2. Computational details

Calculations had been carried out using Gaussian 03 program [19]. The geometries of $XH\cdots NH_3$ systems, neutral and anion, were initially optimized using the density functional theory (DFT)

* Corresponding author at: School of Chemical Engineering, Taishan Medical University, Taian, Shandong 271000, China. Tel.: +86 538 6236121.
E-mail address: donglihua1976@163.com (L.H. Dong).

2210-271X/$ - see front matter © 2012 Elsevier B.V. All rights reserved.
doi:10.1016/j.comptc.2012.01.011

method with a hybrid B3LYP functional [20,21] and the 6-31++G** basis set [22,23]. Five d functions were used on heavy atoms. The extended basis set of 6-31++G**(5d) had been used for the anionic states in previous studies and had been demonstrated through comparison with the second-order Møller Plesset (MP2) predictions [5,7,11,24]. The most accurate electronic energies for the neutral and anionic complexes were calculated at the B3LYP/6-31++G**(6d,7f) level of theory. The electron vertical detachment energies (VDEs) were derived for the anion systems to monitor whether they were vertically bond. The value of VDE, which could be used to assess the trend of PT, was defined as the difference between the energy of anion and the corresponding single point (SP) energy. Furthermore, potential energy surfaces (PESs) for the neutral and anionic states were also scanned along PT pathway at B3LYP/6-31++G**(5d) level.

3. Results and discussion

3.1. Validation of calculations

The reliability of the B3LYP/6-31++G**(5d) method for the XH···NH_3 system has been validated by the anionic system of ClH···NH_3. Firstly, we have fully optimized the $(ClH\cdots NH_3)^-$ structure at the same level. Then, the corresponding energies were calculated at B3LYP/6-31++G**(6d,7f) level. The corresponding bond distances and VDE value are given in Fig. 1. The distance of Cl···H is 1.90 Å and H···N is 1.10 Å. Obviously, with the attachment of an electron, the proton in Cl···H···N has transferred to N atom. This is consistent with the previous work of Gutowski et al. [14]. Our VDE value is 14.63 kcal/mol and consistent with the experiment value of 0.541 ± 0.01 eV (about 12.48 ± 0.23 kcal/mol) and computed value of 0.512 eV (about 11.81 kcal/mol) at CCSD(T)/aug-cc-pvdz level [14]. Such small differences indicate that our method is reliable for describing geometries for anionic XH···NH_3 systems. Therefore, in the following calculations, the B3LYP/6-31++G**(5d) method was used for optimizations of the (XH···NH_3) (X = F, Br, HS, and HCOO) systems. The distances of the optimized geometries and PESs (neutral and anion) are schematic in Figs. 2 and 3 respectively. The values of dipole moment for the neutral complexes are shown in Table 1.

3.2. Degree of proton transfer for (XH···NH_3) (X = F, Br, HS, and HCOO) systems

Upon an electron attachment, the equilibrium F1···N3 distance for anion $(FH\cdots NH_3)^-$ is 2.55 Å (Fig. 2a), which is 0.06 Å shorter than that of the neutral complex, (FH···NH_3). The F1–H2 valence bond distance increases to 1.00 Å, which is 0.03 Å longer than that in neutral, and the distance between H2 and N3 decreases to 1.55 Å. Analysis of F1···H2···N3 distance in anion and neutral indicates that although no PT occurs from HF to NH_3 upon an electron attachment, the valence bond F1–H2 and the hydrogen bond (HB) H2···N3 has been elongated and shortened respectively. Clearly, the trend of PT has been induced upon attachment of an excess electron, which could be seen from the PES in Fig. 3a. It indicates that not only the neutral (FH···NH_3) but also the anion $(FH\cdots NH_3)^-$ surface exhibits a well that corresponds to a hydrogen-bonded complex. Although the PES becomes very flat upon an excess electron attachment, the proton is still coordinated to F1 in $(FH\cdots NH_3)^-$.

For (BrH···NH_3) system in Fig. 2b, the valence bond Br1–H2 increases from 1.55 Å in neutral complex to 2.06 Å in anionic complex, while the HB distance H2–N3 decreases from 1.54 Å to 1.09 Å. Such changes in equilibrium geometries indicate that a new H2–N3 valence bond has been formed in anionic complex. Therefore, PT from HBr to NH_3 is complete upon an excess electron attachment and this process may be easily understood by examining the PESs in Fig. 3b. The neutral surface (black line) shows a well that corresponds to a hydrogen-bonded complex, namely, (BrH···NH_3). On the same distance scale, the corresponding surface of anion exhibits a well at the proton-transferred state, $(Br^-NH_4^+)^-$. It is obvious that the Br1···H2···N3 proton coordinates to Br1 in the neutral and to N3 in the anion. Therefore, the formation of $(Br^-NH_4^+)^-$ should be similar to that of $(NH_4)^0Cl^-$ [14]. Since only one minima is founded in this plot, the PT from HBr to NH_3 is barrier-free upon an electron attachment.

In ($H_2S\cdots NH_3$) system (Fig. 2c), with an electron attachment, the valence bond S1–H2 increases from 1.37 Å in neutral to 1.40 Å in anion, and the HB (H2···N3) decreases from 2.13 Å to 1.89 Å. In this case, $(H_2S\cdots NH_3)^-$ is still a hydrogen-bonded anionic complex, $H_2S\cdots NH_3^-$, and the S1···H2···N3 proton coordinates to S1. The PES of the neutral in Fig. 3c indicates that the curve of anionic $(H_2S\cdots NH_3)^-$ becomes quite flatter, in which two wells are found in this plot. The smooth curve reveals that the proton is able to localize at either side of the two atoms S1 or N3. The transition state (TS) and proton-transferred state (product) are obtained and shown in Fig. 4. In the TS, the S1–H2 distance becomes 1.64 Å, and H2–N3 decreases to 1.35 Å. The proton H2 is not in the center of S1···N3 distance but a little closer to N3 atom. Moreover, vibration analysis shows this stationary point has only one imaginary frequency (809.32i), indicative of a true transition state. For the product, the S1···H2 and H2–N3 distances are 1.93 Å and 1.13 Å, respectively. It is evident that the previous S1–H2 valence bond

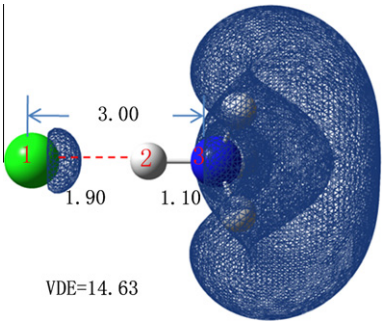

Fig. 1. Geometry of the optimized anionic $(ClH\cdots NH_3)^-$: distance in angstrom and energy in kcal/mol.

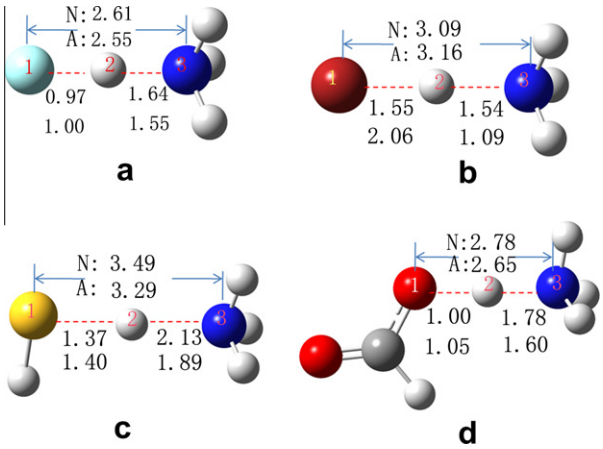

Fig. 2. Schematic diagram of distance changes during the hydrogen exchange process: (a) for FH···NH_3; (b) for BrH···NH_3; (c) for $H_2S\cdots NH_3$; (d) for HCOOH···NH_3. In each group, the values in the upper line show the bond lengths of the neutral (N) complex (XH···NH_3), and in the lower line for the anionic (A) complex. Distances in Angstrom.

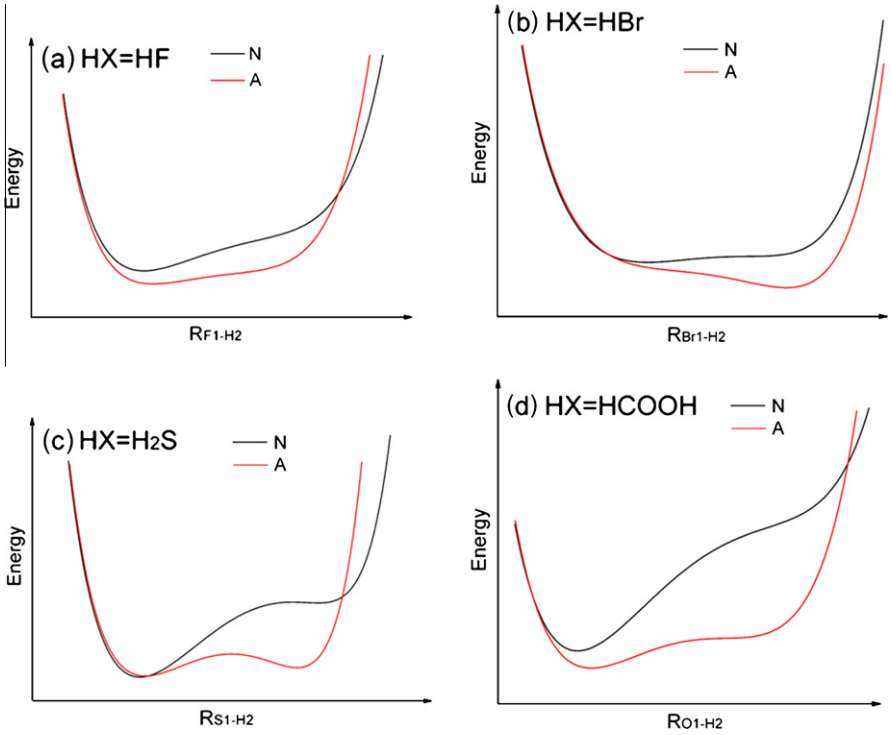

Fig. 3. Potential energy surfaces (PESs) along the proton transfer pathway for the neutral (N) and anionic (A) forms, $XH\cdots NH_3$ and $(XH\cdots NH_3)^-$, respectively.

Table 1
Dipole moment (μ, unit in Debye) of the neutral ($XH\cdots NH_3$), where X = F, Br, HS, and HCOO, determined at the B3LYP/6-31++G**(5d) level.

Geometry	($FH\cdots NH_3$)	($BrH\cdots NH_3$)	($HSH\cdots NH_3$)	($HCOO–H\cdots NH_3$)
μ	4.78	5.07	3.19	4.42

has broken and a new valence bond H2–N3 has been formed. However, for the formation of this proton-transferred state, there is an energy barrier of 1.76 kcal/mol (see Fig. 4). In addition, the energy of the proton-transferred state is 0.84 kcal/mol higher than that of the untransformed state (reactant). Therefore, the intermolecular PT for $(H_2S\cdots NH_3)^-$ is not BFPT.

The geometries and PESs for X = HCOO system are shown in Figs. 2d and 3d, respectively. Analysis reveal that the corresponding changes of the geometries as well as the trends of PESs are similar to that of X = F. It means that the valence bond X–H2 has been elongated and the HB H2···N3 has been shortened upon an excess electron attachment. Only one minima is found in PES, in which the O1···H2···N3 proton still coordinates to O1 side. Thus, intermolecular PT has not occurred with the attachment of excess electron for the $(HCOOH\cdots NH_3)^-$.

The excess electron spin density distributions for the $(XH\cdots NH_3)^-$ (X = F, Br, HS, and HCOO) systems are similar to that of $(ClH\cdots NH_3)^-$ (see Fig. 1) which are not shown. The unpaired electron is always localized on the ammonia end of the $XH\cdots NH_3$ complex.

The possibility of PT for $XH\cdots NH_3$ complex qualitatively depends on the energy difference between the protonation of the anion $(NH_3)^-$ and deprotonation of HX. For $(BrH\cdots NH_3)^-$ complex, the product of PT is $(Br^-NH_4^+)^-$, with the N3 atom hydrogenated and the Br deprotonated. Calculations reveal that deprotonation of HBr requires the energy of 325.32 kcal/mol, while the protonation of $(NH_3)^-$ provides an energy of 339.12 kcal/mol. Therefore, besides enough energy for the PT process, there are extra energies

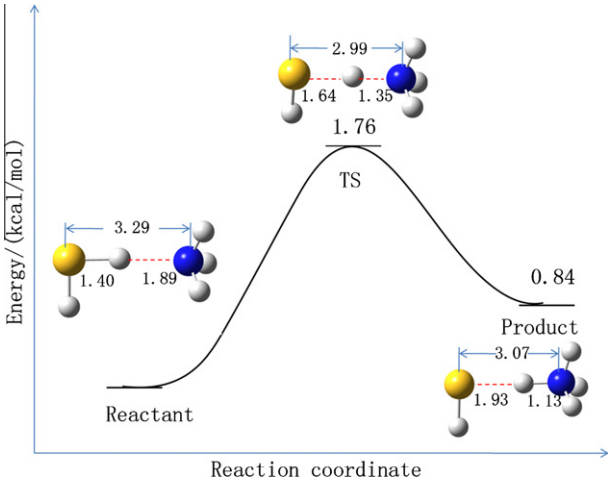

Fig. 4. The stationary points for the intermolecular proton transfer of $(H_2S\cdots NH_3)^-$ system along reaction pathway. Energy in kcal/mol and distances in angstrom.

to release. However, deprotonations of HF, H_2S and HCOOH require energies of 371.29, 353.05, and 343.34 kcal/mol respectively. Each of these values is much larger than that of the energy provided by protonation of the ammonia anion. Thus, it is difficult for PT in these corresponding anionic complexes.

3.3. Degree of proton transfer for $(H_2O)_n(FH\cdots NH_3)^-$ and $(H_2O)_n(HCOOH\cdots NH_3)^-$

It is known that ammonia and hydrogen chloride cannot react with each other under isolated conditions [25–27]. However, in the aqueous solution, the reaction for HCl and NH_3 is almost instantaneous. That is to say, the external factors, such as water, may play a vital role on assisting PT from HCl to NH_3. Besides, it

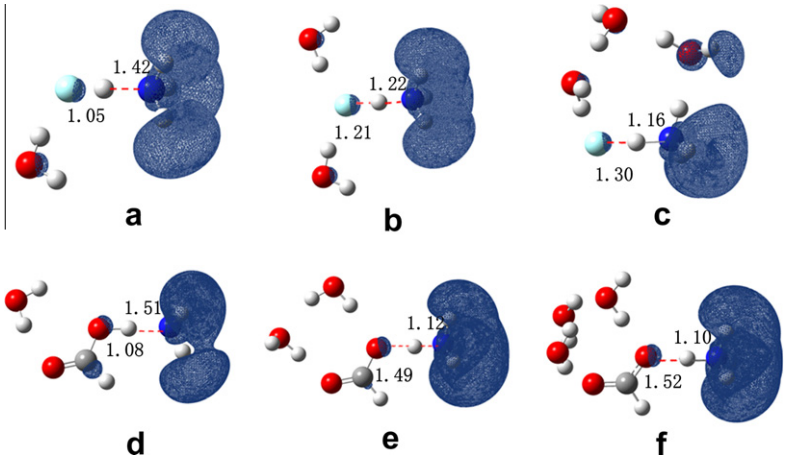

Fig. 5. The optimized anionic clusters of $(H_2O)_n(FH\cdots NH_3)^-$ (a–c) and $(H_2O)_n(HCOOH\cdots NH_3)^-$ (d–f), where n = 1–3. Besides, the excess electron spin density distributions are shown for each structure. Distances in angstrom.

had been shown that PT could occur in the gas phase in the presence of only a few water molecules. We have mentioned that the excess electron could not drive PT in $(FH\cdots NH_3)$ and $(HCOOH\cdots NH_3)$ complexes. Here, calculations were carried out in order to investigate the influence of solvent conditions on PT process in these two clusters.

Calculations had been performed on a series of clusters for $(H_2O)_n(F{-}H\cdots NH_3)^-$ and $(H_2O)_n(HCOO{-}H\cdots NH_3)^-$, where n = 1–3. The spin density distributions and equilibrium distances for these clusters were obtained at B3LYP/6-31++G**(5d) level and shown in Fig. 5. Besides, the PESs along the PT pathway for each cluster were also derived at this level and shown in Fig. 6.

Fig. 5a–c shows the changes of distance (F1–H2, H2···N3 and F1···N3) for $(H_2O)_n(F{-}H\cdots NH_3)^-$ clusters when n = 1–3. The corresponding PESs are represented in Fig. 6a. When n = 1, the valence bond distance F1–H2 increases from 1.00 Å in $(F{-}H\cdots NH_3)^-$ to 1.05 Å in $(H_2O)(F{-}H\cdots NH_3)^-$ and the HB distance H2···N3 decreases from 1.55 Å in $(FH\cdots NH_3)^-$ to 1.42 Å. Obviously, the proton in the $(H_2O)(F{-}H\cdots NH_3)^-$ cluster remains untransformed. Fig. 6a shows that PES of one water molecule system (black line) still exhibits one minima that corresponds to the hydrogen-bonded complex, indicating that the F1···H2···N3 proton coordinates to F1. When the second water molecule is brought into $(F{-}H\cdots NH_3)^-$, compared with one water molecule system, the equilibrium F1–H2 distance increases to r(F1–H2) = 1.21 Å, while the H2···N3 distance decreases to 1.22 Å. Thus, the F1···H2···N3 proton has moved to N3 to some extent. Compared with the PES of n = 1, the PES of n = 2 (red line) only result in a relatively flatter pathway for PT. When n = 3, the valence bond F1···H2 distance reaches 1.30 Å and the HB distance H2–N3 decreases to 1.16 Å respectively. Such an equilibrium geometry reveals that the valence bond F1–H2 has no longer in existence and a new valence bond H2–N3 has been formed. Clearly, the F1···H2···N3 proton has been coordinated to N3. Therefore, this cluster $(H_2O)_3(F^-NH_4^+)^-$ should be a proton-transferred state, which can be seen from the PES in Fig. 6a (green line). There is a deep well that corresponds to the proton-transferred state, $(H_2O)_3(F^-NH_4^+)^-$.

Fig. 5d–f gives the distance changes (O1–H2, H2···N3 and O1···N3) for $(H_2O)_n(HCOO{-}H\cdots NH_3)^-$ clusters when n = 1–3, respectively. The corresponding PESs are represented in Fig. 6b. Comparing with $(HCOO{-}H\cdots NH_3)^-$ anion, the O1–H2 valence bond for $(H_2O)(HCOO{-}H\cdots NH_3)^-$ anion increases to 1.08 Å and the HB distance decreases to 1.51 Å respectively. Obviously, this anion exists as a hydrogen-bonded complex, $(H_2O)(HCOO{-}H\cdots NH_3)^-$, which could be shown from the position of the well in Fig. 6b. when n = 2 (Fig. 5e), the intermolecular PT occurs because the

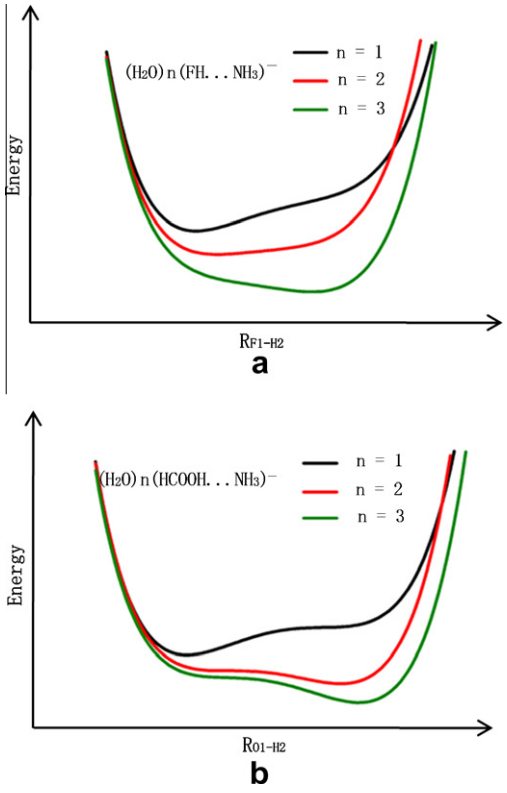

Fig. 6. Potential energy surfaces along the proton transfer pathway for $(H_2O)_n(FH\cdots NH_3)^-$ (a) and $(H_2O)_n(HCOOH\cdots NH_3)^-$ (b) clusters, where n = 1–3.

O1···H2 distance changes to 1.49 Å and H2–N3 to 1.12 Å, which reveals that the valence bond O1–H2 is no longer in existence and a new valence bond H2–N3 has been formed. The corresponding PES (n = 2, red line) exhibits a well and indicates a proton-transferred state, $[(H_2O)_2(HCOO^-NH_4^+]^-$. When the number of water molecules increases to three, the O1···H2···N3 proton in $(H_2O)_3(HCOO{-}H\cdots NH_3)^-$ is closer to N3 than that in cluster $(H_2O)_2(HCOO{-}H\cdots NH_3)^-$, with a more deep well in Fig. 6b (green[1] line).

[1] For interpretation of color in Figs. 1–6, the reader is referred to the web version of this article.

Table 2
Selected bond lengths for the optimized anionic $(XH\cdots NH_3)^-$, $(H_2O)_n(FH\cdots NH_3)^-$, and $(H_2O)_n(HCOOH\cdots NH_3)^-$ clusters calculated at B3LYP/6-31++G**(5d)level.

Complexes	r(H–X)	r^0(H–X)	r(N···H)	r^0(N–H)	ρ_{PT}
$(FH\cdots NH_3)^-$	1.00	0.93	1.55	1.05	−0.43
$(HCl\cdots NH_3)^-$	1.90	1.29	1.10	1.05	0.56
$(BrH\cdots NH_3)^-$	2.07	1.42	1.09	1.05	0.61
$(H_2S\cdots NH_3)^-$	1.40	1.35	1.89	1.05	−0.79[a]
$(HCOOH\cdots NH_3)^-$	1.05	0.97	1.60	1.05	−0.47
$(H_2O)(FH\cdots NH_3)^-$	1.05	0.93	1.42	1.05	−0.25
$(H_2O)_2(FH\cdots NH_3)^-$	1.21	0.93	1.22	1.05	0.11
$(H_2O)_3(FH\cdots NH_3)^-$	1.31	0.93	1.16	1.05	0.27
$(H_2O)(HCOOH\cdots NH_3)^-$	1.08	0.97	1.51	1.05	−0.35
$(H_2O)_2(HCOOH\cdots NH_3)^-$	1.49	0.97	1.12	1.05	0.45
$(H_2O)_3(HCOOH\cdots NH_3)^-$	1.53	0.97	1.10	1.05	0.51

[a] This value corresponds to the proton untransformed state; for the proton-transferred state, $(HS^-\cdots NH_4^+)^-$, the corresponding ρ_{PT} value is 0.50.

Additionally, the excess electron spin density distributions of the optimized clusters, $(H_2O)_n(F–H\cdots NH_3)^-$ and $(H_2O)_n(HCOO–H\cdots NH_3)^-$, are shown in Fig. 5. It could be seen that excess electron is also localized on Rydberg orbitals in all anionic complexes and which is similar to that in $(ClH\cdots NH_3)^-$. However, the spin distributions of the hydrogen-bonded and proton-transferred states are different. For the proton untransformed structures, such as $(H_2O)_n(F–H\cdots NH_3)^-$ (where $n = 1$ and 2) and $(H_2O)(HCOO–H\cdots NH_3)^-$, spin density surfaces are relatively dispersive. For the proton-transferred states, such as $(H_2O)_3(HF\cdots NH_3)^-$ and $(H_2O)_n(HCOOH\cdots NH_3)^-$ (where $n = 2$ and 3), spin density surfaces are centralized together. Thus, the spin distributions provide another scale to access PT. On the same scale, dispersive electron spin distributions correspond to an untransformed structure, while centralized electron spin distribution correspond to a proton-transferred state.

For aforementioned structures, the attachment of an excess electron results in an elongation of H–X bond and a corresponding decrease of N···H distance. A single "proton-transfer parameter" (ρ_{PT}) could be used to describe the simultaneous changes in these distances [28]. The relationship is shown in the following equation:

$$\rho_{PT} = [r(\mathrm{H—X}) - r^0(\mathrm{H—X})] - [r(\mathrm{N}\cdots\mathrm{H}) - r^0(\mathrm{N—H})] \quad (1)$$

where r^0(H–X) and r^0(N–H) refer to the H–X and N–H bond lengths in free HX and protonated ammonia $(H–NH_3)^+$ or ammonia anion $(H–NH_3)^0$, respectively. The distances r(H–X) and r(N···H) refer to the valence bond and HB distances in the complexes of interest, respectively. Therefore, this parameter (ρ_{PT}) assesses the changes of these bonds [29]. When r(H–X) = r^0(H–X) and r(N···H) > r^0(N–H), the proton coordinates to X radical and $\rho_{PT} < 0$. The corresponding anion is a hydrogen-bonded species. When the proton is transferred to N, the length of H–X is elongated and N···H distance decreases, therefore the value of ρ_{PT} changes from negative to positive. When the stretch of the valence bond H–X is equal to the elongation of hydrogen bond N–H, then $\rho_{PT} = 0$. Values of ρ_{PT} for anions calculated from the optimized structures are listed in Table 2. For $(XH\cdots NH_3)^-$ clusters, only $(HCl\cdots NH_3)^-$ and $(BrH\cdots NH_3)^-$ have strongly positive ρ_{PT} values, indicative of a complete degree for PT. Values of ρ_{PT} for $(XH\cdots NH_3)^-$ (X = F, HS, and HCOO) are strongly negative, indicating that no PT occurs in these species and these complexes are hydrogen-bonded. Here, X = HS refers to anion $(H_2S\cdots NH_3)^-$ where the S1···H2···N3 proton coordinates to S1, $(HS–H\cdots NH_3)^-$. However, when proton coordinates to N3, there is a positive value of ρ_{PT} (see note in Table 2), indicative of a proton-transferred form, $(HS^-NH_4^+)^-$. Furthermore, the trends for PT are related to the acidity of HX moiety, which is similar to a previous work of intermolecular proton transfer in anionic complexes of uracil with alcohols [24]. They suggested that the structures of the anionic complexes uracil–alcohols (labeled aAnU) evolved systematically as the gas-phase acidity of different alcohols increased. In our system, the values of ρ_{PT} vary from negative to positive from HF, HCl to HBr, revealing that increasing acidity of HX moiety is also accompanied with increased proton-transferred trend. Additionally, analysis of ρ_{PT} values reveal that the clusters of $(H_2O)_n(H–F\cdots NH_3)^-$ and $(H_2O)_n(HCOO–H\cdots NH_3)^-$, undergo a obvious transition from hydrogen-bonded ($\rho_{PT} < 0$) to proton-transferred ($\rho_{PT} > 0$) states with increased number of water molecules.

Table 3
Electron vertical detachment energies (VDEs) of the optimized anions $(XH\cdots NH_3)^-$ determined at the B3LYP/6-31++G**(6d,7f) level, unit in kcal/mol.

Geometries	VDE
$[(HF)(NH_3)]^-$	0.01
$[(HBr)(NH_3)]^-$	16.60
$[(H_2S)(NH_3)]^-$	12.56
$[(HCOOH)(NH_3)]^-$	0.01

Note: Value in parenthesis corresponds the state that proton is coordinated to N3, $(HS^-\cdots NH_4^+)^-$.

It is known that the smaller values of VDE correspond to hydrogen-bonded states and PT does not occur, while larger values of VDE correspond to a proton-transferred state [6]. In this study, the VDE value of the corresponding anionic $(XH\cdots NH_3)^-$ complexes are summarized in Table 3. For X = F, the corresponding anion, which is hydrogen-bonded complex, has a small VDE value of 0.01 kcal/mol. When X refers to Br, the VDE value becomes 16.60 kcal/mol and the anionic complex is a proton-transferred geometry. Besides, our calculated VDE value for anionic $(ClH\cdots NH_3)^-$ complex is 14.63 kcal/mol (see Fig. 1). It is obvious that VDE values for $(XH\cdots NH_3)^-$ complexes evolve as the gas-phase acidity of HX (from HF, HCl to HBr) increases. Moreover, for X = HS, the VDE value is 12.56 kcal/mol when the S1···H2···N3 proton coordinates to N3. As to the X = HCOO, only a small VDE (0.01 kcal/mol) value is obtained. Clearly, the values of VDE portray a picture in which increasing acidity of HX moiety is accompanied with increased proton-transferred state.

4. Conclusions

In the present study, the influence of an electron attachment to PT of heterodimers $XH\cdots NH_3$ (X = F, Cl, Br, HS, and HCOO) complexes were studied systematically with DFT method.

Two kinds of minima can be found in the anionic $(XH\cdots NH_3)^-$ systems. One kind of anionic complex is $X—H\cdots NH_3^-$, describing a hydrogen bond between an intact HX and anionic ammonia (NH_3^-), such as $F—H\cdots NH_3^-$, $HS—H\cdots NH_3^-$, and $HCOO—H\cdots NH_3^-$. The other kind is $X^-\cdots NH_4$, which describing as a consequence of the proton transfer. The anionic complexes with BFPT possess only one minimum, such as $Cl^-\cdots NH_4$ and $Br^-\cdots NH_4$. The anionic complexes without BFPT can have only one ($F—H\cdots NH_3^-$ and $HCOO—H\cdots NH_3^-$) or two minima ($HS—H\cdots NH_3^-$ and $HS^-NH_4^+$). In the latter case, there is a transition state with an energy barrier of 1.76 kcal/mol.

For the hydrogen bond complex of $F—H\cdots NH_3^-$ and $HCOO—H\cdots NH_3^-$, when solvent is considered as the environmental conditions, degree of PT becomes larger. Analysis indicates that excess electron, indeed, could drive PT in $(H_2O)_n(FH\cdots NH_3)^-$ and $(H_2O)_n(HCOOH\cdots NH_3)^-$ clusters. The minimum number of water molecules is three for the former and two for the latter.

References

[1] R. Barrios, P. Skurski, J. Simons, Mechanism for damage to DNA by low-energy electrons, J. Phys. Chem. B 106 (2002) 7991–7994.

[2] A.F. Jalbout, L. Adamowicz, Dipole-bound anions to adenine–imidazole complex. Ab initio study, J. Phys. Chem. A 105 (2001) 1071–1073.
[3] S.G. Stepanian, A.F. Jalbout, C.S. Hall, L. Adamowicz, Uracil–adenine dimer connected by an excess electron, J. Phys. Chem. A 107 (2003) 7911–7914.
[4] O. Dolgounitcheva, V.G. Zakrzewski, J.V. Ortiz, Anionic and neutral complexes of uracil and water, J. Phys. Chem. A 103 (1999) 7912–7917.
[5] M. Haranczyk, R. Bachorz, J. Rak, M. Gutowski, D. Radisic, S.T. Stokes, J.M. Nilles, K.H. Bowen, Excess electron attachment induces barrier-free proton transfer in binary complexes of uracil with H_2Se and H_2S but not with H_2O, J. Phys. Chem. B 107 (2003) 7889–7895.
[6] M. Haranczyk, I. Dabkowska, J. Rak, M. Gutowski, J.M. Nilles, S. Stokes, D. Radisic, K.H. Bowen, Excess electron attachment induces barrier-free proton transfer in anionic complexes of thymine and uracil with formic acid, J. Phys. Chem. B 108 (2004) 6919–6921.
[7] M. Gutowski, I. Dabkowska, J. Rak, S. Xu, J.M. Nilles, D. Radisic, K.H. Bowen, Barrier-free intermolecular proton transfer in the uracil–glycine complex induced by excess electron attachment, Eur. Phys. J. D 20 (2002) 431–439.
[8] I. Dabkowska, J. Rak, M. Gutowski, J.M. Nilles, S.T. Stokes, D. Radisic, K.H. Bowen, Barrier-free proton transfer in anionic complex of thymine with glycine, Phys. Chem. Chem. Phys. 6 (2004) 4351–4357.
[9] I. Dabkowska, J. Rak, M. Gutowski, J.M. Nilles, S.T. Stokes, K.H. Bowen, Barrier-free intermolecular proton transfer induced by excess electron attachment to the complex of alanine with uracil, J. Chem. Phys. 120 (2004) 6064–6071.
[10] R.A. Bachorz, M. Haranczyk, I. Dabkowska, J. Rak, M. Gutowski, Anion of the formic acid dimer as a model for intermolecular proton transfer induced by a pi(*) excess electron, J. Chem. Phys. 122 (2005) 204304–204310.
[11] D. Radisic, K.H. Bowen, I. Dabkowska, P. Storoniak, J. Rak, M. Gutowski, AT base pair anions versus (9-methyl-A)(1-methyl-T) base pair anions, J. Am. Chem. Soc. 127 (2005) 6443–6450.
[12] M. Haranczyk, M. Gutowski, Valence and dipole-bound anions of the most stable tautomers of guanine, J. Am. Chem. Soc. 127 (2005) 699–706.
[13] T.M. Lowry, The uniqueness of hydrogen, Chem. Ind. (London) 42 (1923) 43–47.
[14] S.N. Eustis, D. Radisic, K.H. Bowen, R.A. Bachorz, M. Haranczyk, G.K. Schenter, M. Gutowski, Electron-driven acid–base chemistry: proton transfer from hydrogen chloride to ammonia, Science 319 (2008) 936–939.
[15] A.C. Legon, The nature of ammonium and methylammonium halides in the vapour phase: hydrogen bonding versus proton transfer, Chem. Soc. Rev. 22 (1993) 153–163.
[16] B. Cherng, F.M. Tao, Formation of ammonium halide particles from pure ammonia and hydrogen halide gases: a theoretical study on small molecular clusters $(NH_3–HX)(n)$ (n = 1, 2, 4; X = F, Cl, Br), J. Chem. Phys. 114 (2001) 1720–1726.
[17] J.A.W. Castleman, J.K.H. Browen, Clusters: structure, energetics, and dynamics of intermediate states of matter, J. Phys. Chem. 100 (1996) 12911–12944.
[18] G.H. Roehrig, N.A. Oyler, L. Adamowicz, Can electron attachment alter tautomeric equilibrium of guanine? Theoretical ab initio study, Chem. Phys. Lett. 225 (1994) 265–272.
[19] M.J. Frisch, G.W. Trucks, H.B. Schlegel, G.E. Scuseria, M.A. Robb, J.R. Cheeseman, J.A. Montgomery Jr., T. Vreven, K.N. Kudin, J.C. Burant, J.M. Millam, S.S. Iyengar, J. Tomasi, V. Barone, B. Mennucci, M. Cossi, G. Scalmani, N. Rega, G.A. Petersson, H. Nakatsuji, M. Hada, M. Ehara, K. Toyota, R. Fukuda, J. Hasegawa, M. Ishida, T. Nakajima, Y. Honda, O. Kitao, H. Nakai, M. Klene, X. Li, J.E. Knox, H.P. Hratchian, J.B. Cross, V. Bakken, C. Adamo, J. Jaramillo, R. Gomperts, R.E. Stratmann, O. Yazyev, A.J. Austin, R. Cammi, C. Pomelli, J.W. Ochterski, P.Y. Ayala, K. Morokuma, G.A. Voth, P. Salvador, J.J. Dannenberg, V.G. Zakrzewski, S. Dapprich, A.D. Daniels, M.C. Strain, O. Farkas, D.K. Malick, A.D. Rabuck, K. Raghavachari, J.B. Foresman, J.V. Ortiz, Q. Cui, A.G. Baboul, S. Clifford, J. Cioslowski, B.B. Stefanov, G. Liu, A. Liashenko, P. Piskorz, I. Komaromi, R.L. Martin, D.J. Fox, T. Keith, M.A. Al-Laham, C.Y. Peng, A. Nanayakkara, M. Challacombe, P.M.W. Gill, B. Johnson, W. Chen, M.W. Wong, C. Gonzalez, J.A. Pople, Gaussian 03, Revision C 02, Gaussian, Inc., Wallingford CT, 2004.
[20] A.D. Becke, Density-functional thermochemistry. III. The role of exact exchange, J. Chem. Phys. 98 (1993) 5648–5652.
[21] C. Lee, W. Yang, R.G. Parr, Development of the Colle–Salvetti correlation-energy formula into a functional of the electron density, Phys. Rev. B 37 (1988) 785–789.
[22] R. Ditchfield, W.J. Hehre, J.A. Pople, Self-consistent molecular-orbital methods. IX. An extended Gaussian-type basis for molecular-orbital studies of organic molecules, J. Chem. Phys. 54 (1971) 724–728.
[23] W.J. Hehre, R. Ditchfield, J.A. Pople, Self-consistent molecular-orbital methods. XII. Further extensions of Gaussian-type basis sets for use in molecular orbital studies of organic molecules, J. Chem. Phys. 56 (1972) 2257–2261.
[24] M. Haranczyk, J. Rak, M. Gutowski, D. Radisic, S.T. Stokes, K.H. Bowen, Intermolecular proton transfer in anionic complexes of uracil with alcohols, J. Phys. Chem. B 109 (2005) 13383–13391.
[25] F.M. Tao, Direct formation of solid ammonium chloride particles from HCl and NH_3 vapors, J. Chem. Phys. 110 (1999) 11121–11124.
[26] R. Cazar, A. Jamka, F.M. Tao, Proton transfer reaction of hydrogen chloride with ammonia: is it possible in the gas phase?, Chem Phys. Lett. 287 (1998) 549–552.
[27] I. Alkorta, I. Rozas, O. Mo, M. Yanez, J. Elguero, Hydrogen bond vs. proton transfer between neutral molecules in the gas phase, J. Phys. Chem. A 105 (2001) 7481–7485.
[28] F.A. van Dijk, A. Dymanus, Hyperfine and Stark spectrum of DBr in the millimeter-wave region, Chem. Phys. 6 (1974) 474–478.
[29] C.S. Brauer, M.B. Craddock, J. Kilian, E.M. Grumstrup, M.C. Orilall, Y.R. Mo, J.L. Gao, K.R. Leopold, Amine–hydrogen halide complexes: experimental electric dipole moments and a theoretical decomposition of dipole moments and binding energies, J. Phys. Chem. A 110 (2006) 10025–10034.